iJRASET
International Journal For Research in Applied Science and Engineering Technology

INTERNATIONAL JOURNAL FOR RESEARCH

IN APPLIED SCIENCE & ENGINEERING TECHNOLOGY

Volume: 7 **Issue:** I **Month of publication:** January 2019

DOI: http://doi.org/10.22214/ijraset.2019.1018

www.ijraset.com

Call: 08813907089 | E-mail ID: ijraset@gmail.com

International Journal for Research in Applied Science & Engineering Technology (IJRASET)
ISSN: 2321-9653; IC Value: 45.98; SJ Impact Factor: 6.887
Volume 7 Issue I, Jan 2019- Available at www.ijraset.com

Structural, Dielectric and Magnetic Properties of Ho and Co Co-substituted $BiFeO_3$ Ceramics

Senbeto Kena Etana[1], P. Vijaya Bhaskar Rao[2]
[1, 2]*Department of Physics, Wollega University, Ethiopia*

Abstract: ***Ceramics of $Bi_{1-x}Ho_xFe_{0.9}Co_{0.1}O_3$(x=0.1, 0.2) have been successfully synthesized by sol-gel technique. The Reitveld refinement XRD data indicated that the rhombohedra pure BFO is transformed to orthorhombic structure with the incorporation of Ho and Co co-doped in BFO ceramic. The increase in the co-substitution content resulted in the decreasing of crystallite size from 26 nm to 15 nm. The results have also revealed that the decrease in crystal parameters, tolerance factor and porosity. The dielectric measurements have shown that with increasing co-doping contents the dielectric constant is enhanced in the lower frequency region and abruptly decreased with frequency and tend to attain constant at higher frequency region. Both the dielectric constant and dielectric loss are increased with temperature up to a transition temperature called Neel temperature, which reveal the magneto-electric coupling. Increasing the co-doping content yields in enhancing spontaneous magnetization from 5.046 emu/g to 17.75 emu/g. The remnant magnetization also enhanced from 0.966 emu/g to 5.55 emu/g with increasing of x from 0.1 to 0.2, respectively. Keywords: nano-particle, multi-ferroics, dielectric constant, dielectric loss, bismuth ferrites, magnetization***

I. INTRODUCTION

$BiFeO_3$ is one of the single phase materials which exhibits both ferroelectric and ferromagnetic properties above room temperature having large ferroelectric Curie temperature ($T_c \sim 1103K$) and G-type anti-ferromagnetic Neel temperature ($T_N \sim 640K$)[1]. BFO has attracted more attention of many researchers for its noble applications in spintronics, information storage like non-volatile memory devices, bubble memory devices, audio/video, in satellite communication etc.[2,3]. Apart from this, BFO by the virtue of its small energy gap, can utilize a wide spectrum of the sunlight in photo induced applications to photovoltaic effect [4] and photo catalytic activity [5, 6].

Recently, many investigators have excited to plan in investigating the simultaneous effect of co-substituting other metal ions in BFO ceramics to improve its multifunctional properties for more potential applications. Previous investigations have demonstrated that co-substitution by Bi^{3+} and Fe^{3+} in BFO with other rare earth ions like Ho^{3+}, Gd^{3+}, Dy^{3+} [7]and transition metal ions like Co^{3+}/Co^{2+}, Ti^{4+}, Mn^{4+}/Mn^{3+}, etc. can significantly improve the structural, dielectric and magnetic properties of BFO ceramics[8,9].

Moreover, extensive investigations have been carried out to adjust the energy gap of BFO ceramics by incorporating the co-doping approach [10]. Zhou et al.(2015) have reported their findings that the saturation magnetization and the optical band gap increased with the increasing of Sm and Mn co-doped BFO, this in turn enhanced the resistivity[10]. Similar reports have been employed by Kuang et al for Y and Co co-doped BFO to increase the optical bang gap that suppressed the enhancement of the resistivity[11].

On the contrary, Kumar and Kar have demonstrated that Ca and Ti co-doped BFO increased the conductivity of the material[12]. Other experimental works have shown that substitution of Gd [13] decreased the conductivity , which in turn enhanced the resistivity of BFO ceramics where as substitution of Mn [14] enhanced the conductivity. Up to our best knowledge, however, the Gd-Mn co-substitution in BFO on the electrical properties have not been reported yet. The co-substituted Gd and La in BFO ceramics have enhanced the dielectric constant up to the maximum of 2500 at 10kHz with increasing the co-doping contents and with increasing La concentration the saturation magnetization increased but the coercive magnetic field decreased [15]. Furthermore, Rai et al. (2013) have demonstrated that with increasing temperature both the dielectric constant and the dielectric loss are increased around transition temperature in the range 125-195^{o}C due to the presence of different types of polarization (electronic, atomic, ionic, dipolar and space-charge).

The room temperature the magnetic behavior of BFO ceramics is due to the Fe sub lattice, which has the G-type anti-ferromagnetic structure having zero net dipole moment. Suresh et al. (2016) demonstrated that La^{3+} and Gd^{3+} in to BFO improved the magnetic properties [16]. Other researchers have demonstrated that magnetization appeared by doping RE ions (RE=La, Nd, Dy) in to BFO ceramics, which attributed to the suppressed of spin cycloid of anti-ferromagnetic structure but not totally destroyed [17]. Hence,

Kumar et al. (2015) concluded that partial substitution should be considered as one of the most effective ways for improving the multiferroic characteristic of G-type anti-ferromagnetic order with a long period of $\sim 62nm$ of BFO.

So in this work, we are interested to dope the rare earth ions in A-site and metallic ions in B-site. Doping of these metallic ions at A-site or B-site, in appropriate chemical stiochiometry can improve the multifunctional properties like magnetization and dielectric, to reduce AC conductivity of the material by suppressing the oxygen vacancies and spiral spin cycloid structure.

II. EXPERIMENTAL DERAILS

Ceramics of $Bi_{1-x}Ho_xFe_{0.9}Co_{0.1}O_3$ (x=0.1, 0.2) are prepared by sol-gel technique. The stoichiometric ratios of $Bi(NO_3)_3.5H_2O$, $Ho(NO_3)_3.5H_2O$, $Fe(NO_3)_3.9H_2O$, $Co(NO_3)_2.6H_2O$ with purity 98% and and citric acid ($C_6H_8O_7$) was used as chelating agent. All these metal nitrates were mixed in 250ml beaks containing amount of doubly de-ionized water and stirred continuously by magnetic stirrer without heating. Equal mole of citric acid was added to the nitrate solution (i.e., one mole of citric acid must be added to one mole of metal nitrate in order to facilitate the reaction). Again the mixed nitrate solution and citric acid are stirred with high velocity to obtain uniform clear solution. Then the solution in the beaker was place on hot plate staying on high velocity magnetic stirrer, heating up to a temperature of 90^oC. 28% ammonia solution (NH_3) was drop wisely added to the solution to control the PH value around neutral with continuous stirring. This was continued until the solution is turned to gel.

The formed gel was poured on to the evaporating dish and placed in hot oven at a temperature of 120^oC for 4 hrs to become dry gel. Then, water evaporation is held by raising the temperature of the dried gel to 220^0C to form powder ash. The ash was gently ground by agate mortar to obtain the fine powder and the powder in high temperature resistance crucible placed in hot electric furnace for pre-sintering at 650^oC for 3hrs in order to remove excess hydrocarbon and some impurities. The powders were again grinded very finely and pressed to the pellet of about 1mm thick and 10mm diameter disks with hydraulic press of 12.5 ton. Finally the pellets were sintered at 850^{o}C for 4 hrs resulting in good densification. For impedance measurement both sides of the surface of the pellet samples were silvered using silver paste and heated at 100^{o}C for 1hr.

The structural and phase identification are characterized by Philips X'Pert PRO3040/60 (with raw data origin *XRDML, at Osmania University) diffracto meter with Cu Kα (λ=0.154nm) as radiation source in wide range of Bragg angle from 20^0 to 60^0 in steps of 0.020 at room temperature. The surface morphology and the elemental composition of the sample was characterized by scanning electron microscope (SEM) and energy dispersive X-ray (EDX), respectively. the dielectric properties were measured using impedance analyzer (Wayne Kerr). Magnetic measurement at room temperature was conducted using vibrating sample magnetometer (VSM, Lakeshore 7407 series).

III. RESULTS AND DISCUSSIONS

A. Structural Analysis

Figure 1.1a &b show the XRD pattern of $Bi_{1-x}Ho_xFe_{0.9}Co_{0.1}O_3$ (x=0.1, 0.2) ceramics calcined at 650^oC for 3 hrs and sintered at 850^oC for 4 hrs. The Reitveld refinement analysis confirmed that the observation of small amount of impurities indicated by ($) associated with $Bi_2Fe_4O_9$ and $Bi_{25}FeO_{40}$. These impurities will lead to the generation of more oxygen vacancies which contribute ac conductivity to the ceramics.

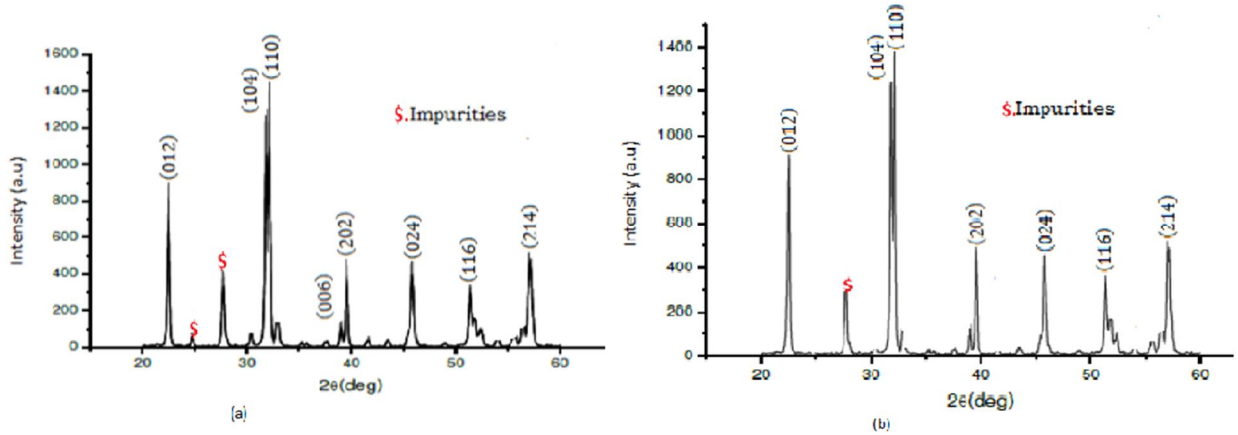

Figure 1. XRD spectra for a) x=0.1 b) x=0.2

In figures 1 a&b, distinct peaks corresponding to the planes (110) and (104); (006) and (202), were observed around 32^0 and 39^0, respectively. All the XRD patterns suggested that (Ho, Co) co-doped give rise to structural transition from rhombohedra to orthorhombic. Similar XRD peaks change upon (Ho, Mn) co-doped were previously reported as a signature of structural transition [18] (*Ye et al, 2015*). The result of the structural distortion is consistent with the reports of reference [19]*Y. Qi, B. Alima and Z. Shefeng (2014*), when Ho^{3+} ion is incorporate in to BFO. The average crystallite size (D) from intense XRD peak is calculated using Debye-Scherer formula of (equation 1).

$$D = \frac{K\lambda}{\beta Cos\theta} \quad (1)$$

K=0.89 is the Scherer constant, λ is the wave length of the X-ray, β is the full width at half maximum (FWHM) and θ is the Bragg angle at which intense peak is occurred. The refined crystal parameters are summarized in Table 1.

Table 1. Refined Crystal structure for $Bi_{1-x}Ho_xFe_{0.9}Co_{0.1}O_3$ (x=0.1, 0.2) ceramics

Sample	Crystallite size (D) (nm)	Lattice parameters	Tolerance factor (t)	x-ray density (g/cm^3)	Measured density (g/cm^3)	Porosity (%)
X=0.1	26.30	a=b=5.572A c=13.65A V=367$(A)^3$	0.884	6.92	6.38	7.8
X=0.2	15.00	a=b=5.546 A c=13.24A V=352.6$(A)^3$	0.879	6.94	6.44	7.3

From Table 1, it is clear that the crystal parameters are decreased as the concentration of the co-doping increased. These values are smaller than the values of BFO (D= 46 nm [20],a=b=5.8 A, c=13.87A, [21]). The decrease of these values are attributed to the smaller ionic radii of the co-substituted ions that led to the contraction of the unit cell and increased the octahedral tilt FO_6, which in turn increase the canting angle of Fe-O-Fe to suppress the anti-ferromagnetic nature of the sample[22]

The estimated x-ray density from equation (2)[23] increase with increasing of co-doping content, while the porosity calculated using equation(3)[24] decrease with the increase of co-substituted BFO due the closed oxygen vacancies.

$$\rho_{x-ray} = \frac{ZM}{N_aV} \quad (2)$$

Z is the number of the molecule per a unit cell, M molecular weight of the compound, Na is the Avogadro number and V is the volume of the unit.

$$Porosity(P\%) = 1 - \frac{\rho_m}{\rho_{x-ray}} \quad (3)$$

ρ_m is the measured density of the sample

B. Dielectric Studies

Figure 2 shows the variation of real dielectric constant (ε') (a) and dielectric loss (loss tanδ)(b) of $Bi_{1-x}Ho_xFe_{0.9}Co_{0.1}O_3$ (x=0.1, 0.2) ceramics with frequency in the range from 1kHz to 1MHz, measured at 360^oC. It is observed that there is an enhancement of the dielectric constant and decreased in dielectric loss with the co-doping content of the samples. The values the dielectric constant and the dielectric loss are sharply decreased with increasing of frequency up to around 10 kHz, then after tend to constant. The value of the dielectric constant for x=0.1 at 1kHz increased from $1.42x10^4$ to the maximum value of $4.54x10^4$ for x=0.2. For this co-doping contents, the dielectric loss is lower compared to x=0.1. The reduction of the dielectric loss with increasing the co-dopants is attributed to the reduction of the bismuth loss which contributed for conduction.

As in Table 1, the increased density of the sample may contribute to the reduction of the dielectric loss. In a pure BFO, the polar activity of the Bi^{3+} is the main contribution fot the observation of polarization and hence dielectric constant [16]. The dielectric dispersion at the lower frequency is attributed to the space charge polarization which arises from oxygen vacancies [25]

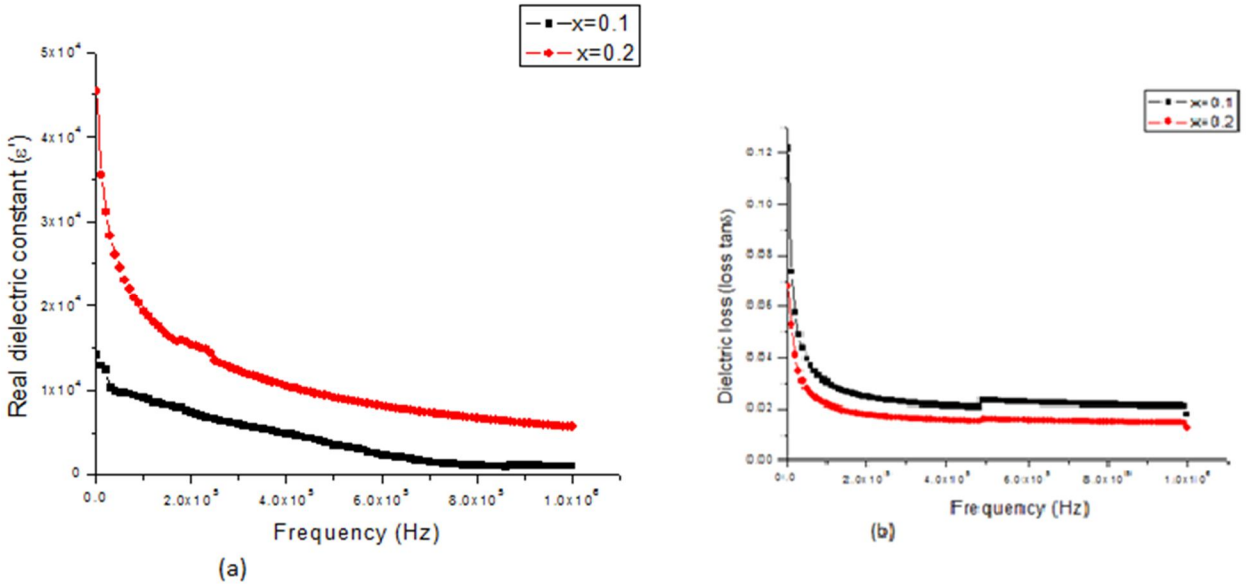

Figure 2 Variation of a) real dielectric constant and b) dielectric loss with frequency

The high value dielectric and low value of the dielectric loss with co-doping samples indicating the lower charge defect [26].
Figures 3 shows variation of dielectric constant (ε') and dielectric loss (tanδ) with temperature ranging from 150°C to 400°C at various frequencies (1kHz, 10 kHz, 50kHz and 1MHz) for x=0.1 (a & b) and x=0.2 (c & d).

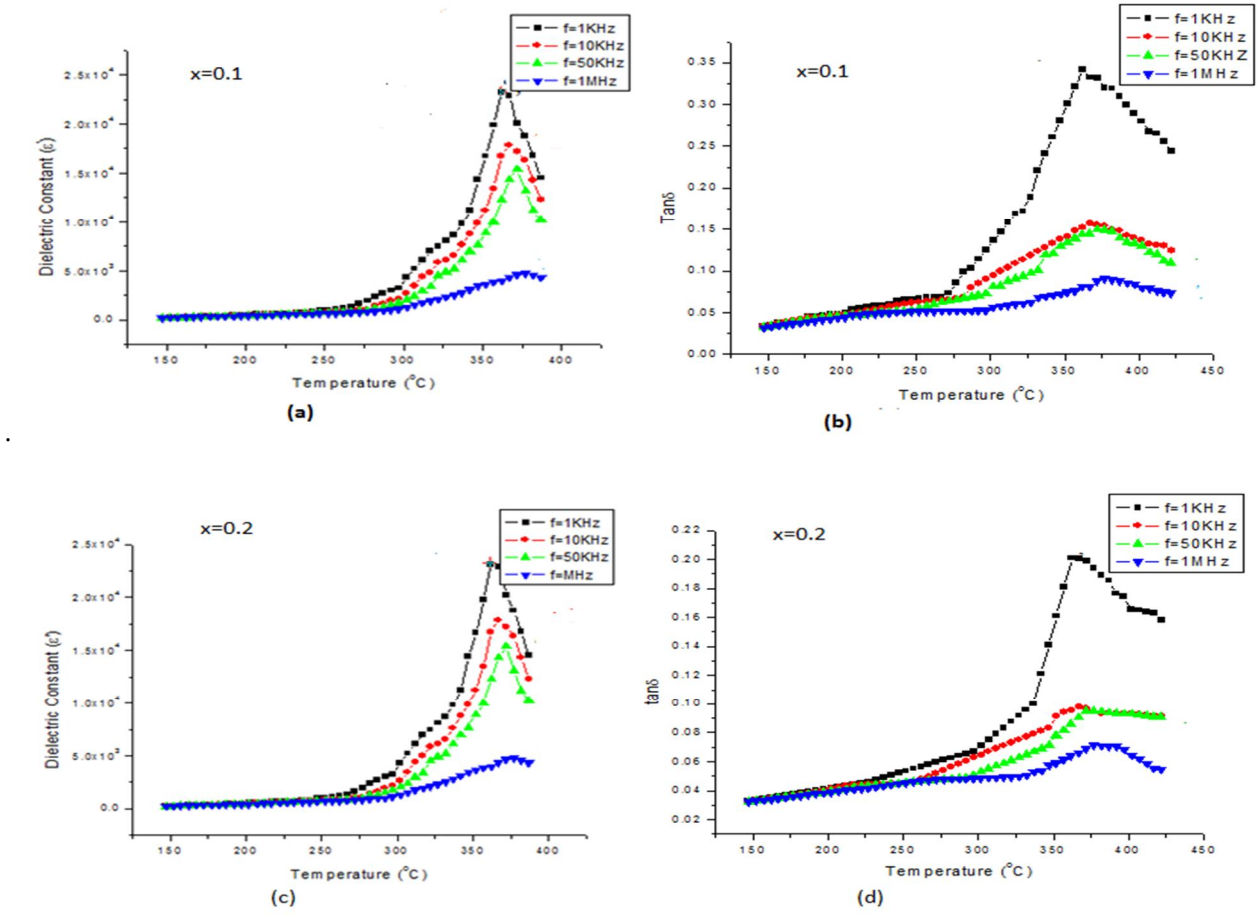

Figure 3 Variation of a) real dielectric constant and b) dielectric loss with temperature

ISSN: 2321-9653; IC Value: 45.98; SJ Impact Factor: 6.887
Volume 7 Issue I, Jan 2019- Available at www.ijraset.com

From ε' versus T (figure 3), the broad peaks are observed around 376^oC for x=0.1 and 378^oC for x=0.2, indicating dielectric anomaly, which is close to the magnetic transition temperature of BFO (370^oC)[27]. This anomaly is attributed to the transition of the sample from anti-ferromagnetic to paramagnetic, which influence of vanishing magnetic order on electric order [28]. For the sample with x=0.2 high dielectric constant peak in the order of 10^4 is observed at 1kHz. In $tan\delta$ versus T plot, broad peaks are observed nearly at around same temperature as in case of dielectric constants.

From the plots, it is clearly seen that the broad peaks are shifted to the higher temperature as the measuring frequency increase. Similar behavior has been observed in the report of Z.X. Cheng et al. (2008)[29] when La is substituted Bi in BFO.

C. Magnetic Studies

Figure 4 shows the room temperature M-H hysteresis loop for $Bi_{1-x}Ho_xFe_{0.9}Co_{0.1}O_3$ (x=0.1, 0.2) ceramics.

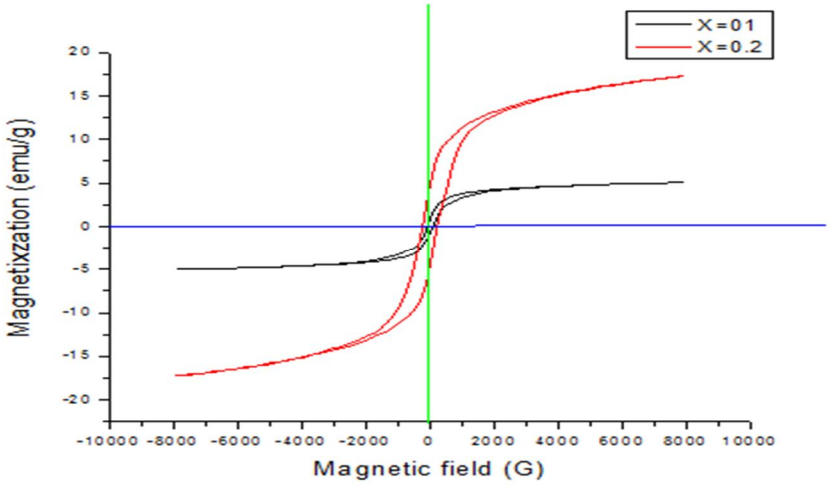

Figure 4 M-H hysteresis loop for $Bi_{1-x}Ho_xFe_{0.9}Co_{0.1}O_3 (x = 0.1, 0.2)$ ceramics

Table 2. Variation magnetic parameters with co-doping

sample	Saturation magnetization, Ms (emu/g)	Remnant magnetization, Mr (emu/g)	Coercive field , Hc (G)
X=0.1	5.046	0.966	126
X=0.2	17.75	5.55	249.82

As seen in Table 2 above, for each co-doping concentration, the measure values of magnetization are much greater than that of the parent BFO, which is 0.0028emu/g[21]. The enhancement of magnetic properties is attributed to the reduction of crystallite size when ions of smaller ionic radii are incorporated in BFO ceramic, a confirmed in XRD result (Table 1) and SEM morphology. All these values are lower than SMSS period of 62nm, which may suppress the spin cycloid anti-ferromagnetic structure and improve the magnetization. The results obtained are in agreement with the results found for the Y and Sc co-doped BFO by A. K. Jena and J. Mohanty (2017).

IV. CONCLUSION

In this work, we have succeeded in preparing $Bi_{1-x}Ho_xFe_{0.9}Co_{0.1}O_3$ nano-particles, (x=0.1, 0.20) using the sol–gel method. The crystal structure of the nano-particles was transformed from rhombohedra (pure BFO) to orthorhombic with increasing doping concentration. The dielectric properties of the co-doped samples were affected by the properties of the substituted ions as well as the crystalline structure of the samples. The co-doping samples were greatly improved the dielectric properties of BFO and suitable amount of $Co^{2+}$and Ho^{3+}ions was high in improving the magnetization of the nano-particles at the same doping concentration. The enhancement of dielectric properties in the lower frequency region is attributed to the suppression of oxygen vacancies.

The values of saturation magnetization (Ms) and remnant magnetization (Mr) significantly increased with increasing co-doping concentrations due to the suppression of spin spiral cycloid structure as a result of the incorporation of smaller ionic radii of the co-substituted ions in BFO ceramic. These results have suggested that the Ho and Co co-doped BFO nano-crystalline is promising for applications in data-storage media.

V. ACKNOWLEDGEMENT

This work was financially supported by Wollega University (Ethiopia). Osmania University supported us in permitting the laboratory room, especially, In-organic chemistry wet lab. The physics department helped us in permitting to use furnace, impedance analyzer. XRD, SEM, EDX, FTIR. University of Hyderabad also helped us to analyze the magnetic properties of our samples.

REFERENCES

[1] P. Pandit, S Satapathy, P. Sharma, P K Gupta, S M. Yusuf and V G Sathe, Structural, Dielectric and multiferroic properties of Er and La substituted $BiFeO_3$ ceramics, Bull. Mater. Sci., Vol. 34, No. 4, pp. 899–905, 2011.

[2] H. Dai, Z. Chen, R. Xue,T. Li et al., Structural and electric properties of polycrystalline $Bi_{1-x}Er_xFeO_3$ ceramics, Ceramics International 39, pp.5373–5378, 2013.

[3] Y.Q. Liu, Y.J. Wang, J. Zhang et al., Effect of Ho substitution on structure and magnetic property of BFO prepared by sol–gel method, Materials Science in Semiconductor Processing 40, pp.787-795,2015.

[4] S.Y. Yang, L.W. Martin, S.J. Byrnes, T.E. Conry et al., Photovoltaic effects in $BiFeO_3$, Applied Physics Letters, 95, 062909, 2009.

[5] F. Gao, X.Y. Chen, K.B. Yin, S. Dong et al., Visible-Light Photocatalytic Properties of Weak Magnetic $BiFeO_3$ Nanoparticles, Advanced Materials, 19, 2889-2892, 2007.

[6] X. Bai, J. Wei, B. Tian, Y. Liu et al., Infante Size Effect on Optical and Photocatalytic Properties in $BiFeO_3$ Nanoparticles, The Journal of Physical Chemistry C, 120, 3595-3601, 2016.

[7] A. Gautam, K. Singh, K. Sen, R.K. Kotnala, M. Singh, Crystal structure and magnetic property of Nd doped $BiFeO_3$ nanocrystallites, Mater. Lett. 65, pp. 591-594, 2011.

[8] H. Singh and K.L. Yadav, Effect of Nb substitution on the structural, dielectric and magnetic properties of multiferroic $BiFe_{1-x}Nb_xO_3$ ceramics, Mater. Chem. Phys.132 pp.17- 21, 2012.

[9] V.R. Palkar, D.C. Kundaliy & S. K. Malik, Effect of Mn substitution on magneto- electric properties of 3bismuth ferrite system, Journal of Applied Physics 93, 7834, 2003.

[10] W. Zhou, H. Deng, H. Cao, J. He, J. Liu, P. Yang, J. Chu , Effects of Sm and Mn co-doping on structural, optical and magnetic properties of $BiFeO_3$ films prepared by a sol–gel Technique, Materials Letters, 144, 93-96, 2015.

[11] D. Kuang, P. Tang, X. Wu, S. Yang, X. Ding, Y. Zhang, Structural, optical and magnetic studies of (Y, Co) co-substituted BiFeO3 thin films, Journal of Alloys and Compounds, 671, 192-199, 2016.

[12] P. Kumar and M. Kar , Effect of structural transition on magnetic and optical properties of Ca and Ti co-substituted $BiFeO_3$ ceramics, Journal of Alloys and Compounds, 584 566-572, ,2014.

[13] R. Guo, L. Fang, W. Dong, F. Zheng, M. Shen, Enhanced Photocatalytic Activity and Ferromagnetism in Gd Doped $BiFeO_3$ Nanoparticles.' The Journal of Physical Chemistry C, 114, 21390-21396, 2010.

[14] S. Chauhan, M. Kumar, S. Chhoker, S.C. Katyal, H. Singh, M. Jewariya, K.L. Yadav, Multiferroic, magnetoelectric and optical properties of Mn doped $BiFeO_3$ nanoparticles, Solid State Communications, 152, 525–529, 2012.

[15] R. Rai M.A.Valente , L.Kholkin S. Sharma, Enhanced ferroelectric and magnetic properties of perovskite structured $Bi_{1-x-y}Gd_xLa_yFe_{1-y}Ti_y$ magnetoelectric ceramics, Journal of Physics and Chemistry of Solids 74, 905–912, 2013.

[16] P. Suresha, P.D.Babuc, S.Srinath, Role of (La,Gd) co-doping on the enhanced dielectric and magnetic properties of $BiFeO_3$ ceramics. Ceramics International42, 4176–4184, 2016.

[17] A.Kumar, P. Sharma, and D.Varshney, Structural and Ferroic Properties of La, Nd, and Dy Doped $BiFeO_3$ Ceramics, Research Article, Journal of Ceramics, 8 pages, 2015.

[18] W.Ye, G.Tan, G. Dong,H.Ren, A. Xia, Improved multiferroic properties in(Ho, Mn) co- doped $BiFeO_3$ thin films prepared by chemical solution deposition, Ceramics International 41, pp.4668–4674, 2015.

[19] Y. Qi, B. Alima and Z. Shifeng, .Lattice distortion of holmium doped bismuth ferrite nano films, Journal of Rare Earths, Vol. 32, No. 9, P. 884-889, 2014.

[20] A.K Sinha, B. Bhushan, D. Rout, R. K. Sharma et al., Structural and magnetic properties of Cr doped $BiFeO_3$ multiferroic nanoparticles, AIP Conference Proceedings 1832, 050088, 2017.

[21] A.K. Jena and J. Mohanty, Enhancing ferromagnetic properties in bismuth ferrites with non-magnetic Y and Sc co-doping, Journal of Materials Science, Materials in Electronics, 2017.

[22] C.H. Yang, D. Kan, I. Takeuchi, V. Nagarajan, J. Seidel, Doping $BiFeO_3$:approaches and enhanced functionality, Phys. Chem. Chem. Phys., vol. 14, pp. 15953, 2012.

[23] B.D. Cullity, Elements of X-ray diffraction (2nd-ed.), Addison-Wesley series, 1978.

[24] S. Ahmad, A. K Muhammad, S.Mansoor et al., The impact of Yb and Co on structural, magnetic, electrical and Photo- catalytic behavior of nanocrystalline multiferroic $BiFeO_3$ particles, Ceramics International 43 pp.16880–16887, 2017.

[25] P. R. Das, B. Pati, B. C. Sutar, R. N. P. Choudhury, Study of Structural and Electrical Properties of a New Type of Complex Tungsten Bronze Electroceramics $Li_2Pb_2Y_2W_2Ti_4V_4O_{30}$, Journal of Modern Physics, 3, 870-880, 2012.

[26] R. Das, T. Sarkar & K Mandal, Multiferroic properties of Ba^{2+} and Gd^{3+}co- doped ferrite: magnetic, ferroelectric and impedance spectroscopic analysis, J. Phys. D, Appl. Phys. 45, 455002, 10, 2012.

[27] B. Kaur, L. Singh, V. A. Reddy et al., AC Impedance Spectroscopy, Conductivity and Optical Studies of Sr doped Bismuth Ferrite Nano-composites, Int. J. Electrochem. Sci., 11, 4120 – 4135, 2016

[28] P.Uniyal & K.L. Yadav, Study of dielectric, magnetic and ferroelectric properties in $Bi_{1-x}Gd_xFeO_3$, Materials Letters 62 2858–2861, 2008.

[29] Z. X. Cheng, A. H. Li, X. L. Wang, S. X. Dou, K. Ozawa, H. Kimura, S. J. Zhang, and T. R. Shrout, Structure, ferroelectric properties, and magnetic properties of the La-doped bismuth ferrite. Journal of Applied Physics 103, 07E507, 2008.

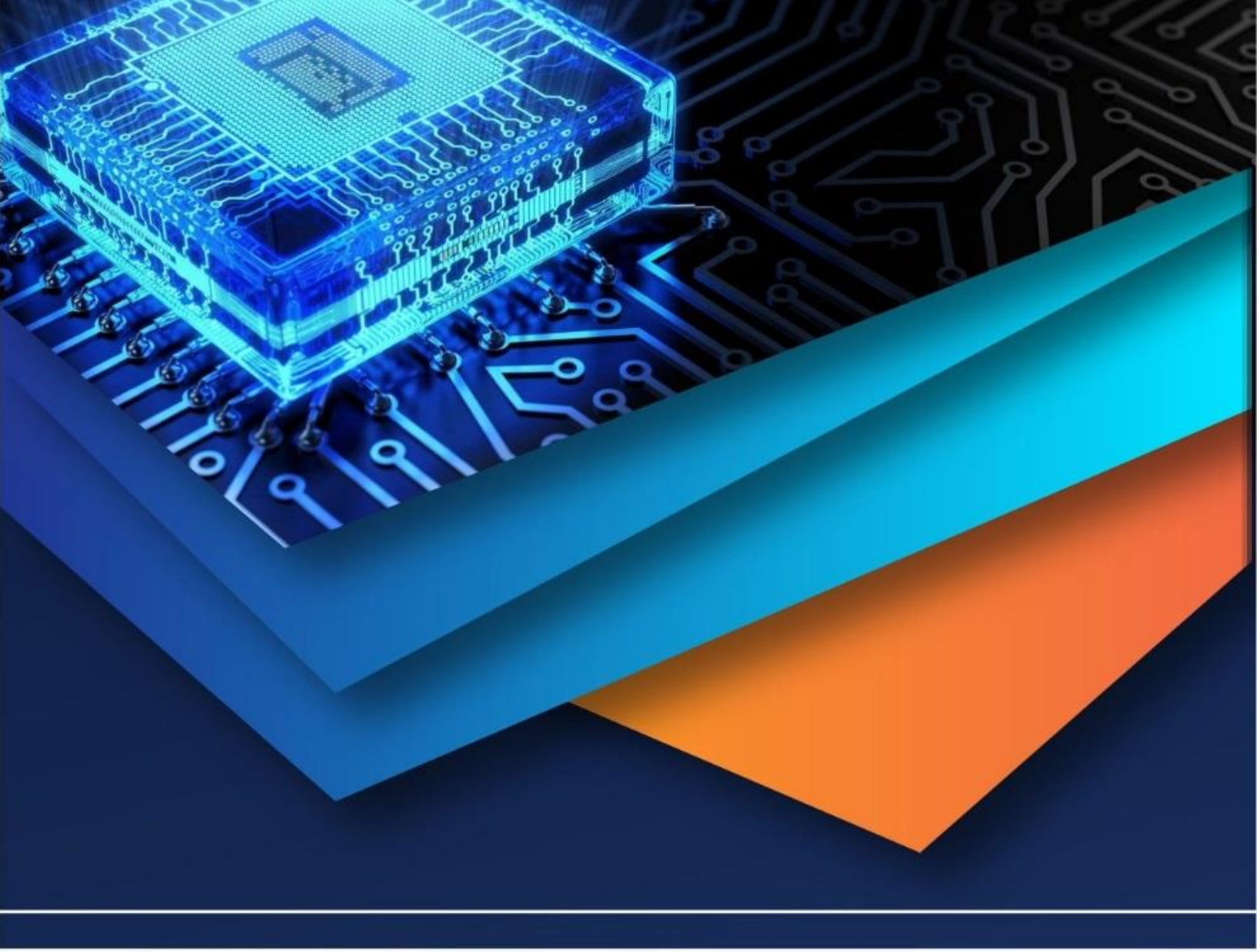

10.22214/IJRASET

45.98

IMPACT FACTOR: 7.129

IMPACT FACTOR: 7.429

INTERNATIONAL JOURNAL FOR RESEARCH

IN APPLIED SCIENCE & ENGINEERING TECHNOLOGY